Title

RpoN (σ54) Is Required for Floc Formation but Not for Extracellular Polysaccharide Biosynthesis in a Floc-Forming Aquincola tertiaricarbonis Strain

Journal

Applied and Environmental Microbiology, 83(14)

ISSN

0099-2240

Authors

Yu, Dianzhen

Xia, Ming

Zhang, Liping

et al.

Publication Date

2017-07-15

DOI

10.1128/aem.00709-17

Peer reviewed

RpoN (σ^{54}) Is Required for Floc Formation but Not for Extracellular Polysaccharide Biosynthesis in a Floc-Forming *Aquincola tertiaricarbonis* Strain

Dianzhen Yu,[a,b] Ming Xia,[a,b] Liping Zhang,[a] Yulong Song,[a] You Duan,[a,b] Tong Yuan,[d,f] Minjie Yao,[c] Liyou Wu,[d] Chunyuan Tian,[e] Zhenbin Wu,[a] Xiangzhen Li,[c] Jizhong Zhou,[d] Dongru Qiu[a]

Institute of Hydrobiology, Chinese Academy of Sciences, Wuhan, China[a] ; University of Chinese Academy of Sciences, Beijing, China[b]; Chengdu Institute of Biology, Chinese Academy of Sciences, Chengdu, China[c] ; Institute for Environmental Genomics, Department of Microbiology and Plant Biology, University of Oklahoma, Norman, Oklahoma, USA[d]; School of Life Sciences and Technology, Hubei Engineering University, Xiaogan, China[e]; College of Life Science, Henan Agricultural University, Zhengzhou, China[f]

ABSTRACT

Some bacteria are capable of forming flocs, in which bacterial cells become self-flocculated by secreted extracellular polysaccharides and other biopolymers. The floc-forming bacteria play a central role in activated sludge, which has been widely utilized for the treatment of municipal sewage and industrial wastewater. Here, we use a floc-forming bacterium, *Aquincola tertiaricarbonis* RN12, as a model to explore the biosynthesis of extracellular polysaccharides and the regulation of floc formation. A large gene cluster for exopolysaccharide biosynthesis and a gene encoding the alternative sigma factor RpoN1, one of the four paralogues, have been identified in floc formation-deficient mutants generated by transposon mutagenesis, and the gene functions have been further confirmed by genetic complementation analyses. Interestingly, the biosynthesis of exopolysaccharides remained in the *rpoN1*-disrupted flocculation-defective mutants, but most of the exopolysaccharides were secreted and released rather than bound to the cells. Furthermore, the expression of exopolysaccharide biosynthesis genes seemed not to be regulated by RpoN1. Taken together, our results indicate that RpoN1 may play a role in regulating the expression of a certain gene(s) involved in the self-flocculation of bacterial cells but not in the biosynthesis and secretion of exopolysaccharides required for floc formation.

IMPORTANCE Floc formation confers bacterial resistance to predation of protozoa and plays a central role in the widely used activated sludge process. In this study, we not only identified a large gene cluster for biosynthesis of extracellular polysaccharides but also identified four *rpoN* paralogues, one of which (*rpoN1*) is required for floc formation in *A. tertiaricarbonis* RN12. In addition, this RpoN sigma factor regulates the transcription of genes involved in biofilm formation and swarming motility, as previously shown in other bacteria. However, this RpoN paralogue is not required for the biosynthesis of exopolysaccharides, which are released and dissolved into culture broth by the *rpoN1* mutant rather than remaining

tightly bound to cells, as observed during the flocculation of the wild-type strain. These results indicate that floc formation is a regulated complex process, and other yet-to-be identified RpoN1-dependent factors are involved in self-flocculation of bacterial cells via exopolysaccharides and/or other biopolymers.

KEYWORDS bacterial floc formation, extracellular polysaccharides, flocculation, RpoN sigma factor, *Aquincola tertiaricarbonis*

INTRODUCTION

Nuisance brown precipitates have been appearing in the tap water from a water supply factory located in Xishui County, Hubei Province, China, for over a decade, and the mechanism underlying the formation of such brown precipitates remains intriguing. Efforts have been made to isolate the bacterial and algal strains that may be responsible for the formation of the brown precipitates, and chlorine bleaching did not overcome the problem. Because the water quality of the river used as a water source is good, a sand filtration process is used to purify the river water that is stored in the deep wells before being distributed as drinking water via water supply pipelines. However, brown precipitates that occurred in the well have been an unresolved nuisance to the local inhabitants. Iron-oxidizing bacteria, such as *Leptothrix* species, are a common nuisance in water wells, though they are not considered a public health hazard (1, 2). We isolated a series of bacterial strains from the water and brown precipitate samples taken from the well and household tap water. We also analyzed the microbial communities in the well water and tap water, as well as in the brown precipitates. The *Leptothrix* sp. bacterium has not been detected in either water or brown precipitate samples, and *Undibacterium* and *Pseudomonas* bacteria seem to be the predominant species in the brown precipitates (data not shown). Under laboratory cultivation conditions, one bacterial isolate, RN12, remarkably formed bacterial flocs that could settle without agitation. This strain has been identified as *Aquincola tertiaricarbonis* by both 16S rRNA gene phylogeny and draft genome sequencing. This strain was present in both water and brown precipitate samples and was subjected to further molecular genetics analyses for the phenotype of floc formation, which may be related to the brown precipitates that occurred in the well and tap water and also a trait desirable for activated sludge-based wastewater treatment. The *Aquincola* strains are capable of degrading gasoline-related contaminants (3–6) and therefore may have great potential in bioremediation because of their floc-forming capability. Recently, it was shown that *Aquincola* species were one of the predominant proteobacteria in a membrane bioreactor (MBR) treating antibiotics-containing wastewater (7). Furthermore, floc-forming bacteria, including *Zoogloea ramigera*, are believed to play a crucial role in the activated sludge process widely used for treatment of municipal sewage and industrial wastewater. The bacterial flocs, suspended in the ambient water and also found in activated sludge, may confer bacterial resistance to the predation of protozoa and other invertebrates and may also be related to

other uncharacterized traits (8). Activated sludge floc formation makes it possible to achieve gravity-based separation of clean effluent from sludge in the settlement tank and also the recycling of settled sludge to an aeration tank for favorable food-to-microbe ratios. We could also take advantage of the floc-forming and contaminant-degrading capacity of *Aquincola* for many biotechnological applications and bioremediation methods, because this bacterium could be readily enriched and harvested, as activated sludge bacteria are. Therefore, we conducted a series of molecular genetics and biochemical studies on the floc formation of the *A. tertiaricarbonis* RN12 strain. We identified a large gene cluster involved in biosynthesis of extracellular polysaccharides and floc formation in strain RN12. The exopolysaccharide biosynthesis gene cluster of *Aquincola* shares many genes with that of *Zoogloea resiniphila* (9). More interestingly, it has also been revealed that an alternative sigma factor, RpoN1 (σ^{54}), one of the four paralogues, is required for bacterial floc formation, though the biosynthesis of exopolysaccharides remained largely unaffected in the *rpoN*-disrupted mutant in this study. Furthermore, some of the identified exopolysaccharide biosynthesis genes seemed not to be regulated by this sigma factor. In addition, the synthesized extracellular polysaccharides were secreted, released, and became dissolved in the culture broth instead of flocculating the bacterial cells to form flocs when the *rpoN1* gene was disrupted. It is shown that floc formation is a regulated complex process, and other yet-to-be identified RpoN1-dependent factors are involved in self-flocculation of bacterial cells. These results provide insights into the regulation of floc formation in *Aquincola*, *Zoogloea*, and other floc-forming bacteria.

RESULTS

Isolation and characterization of a floc-forming *A. tertiaricarbonis* strain.A series of culture media, including LB and R2A, were used to isolate the bacterial strains from the wells affected by brown flocculent precipitates (see Fig. S1 in the supplemental material). Only RN12, one strain among the bacterial isolates, could form flocs in the R2A broth. The 16S rRNA gene sequence-based phylogenetic analyses demonstrated that RN12 was very close to the tertiary butyl moiety-degrading bacterium *A. tertiaricarbonis* type strain L10, with 99% sequence identity (Fig. S2A) (10). The draft genome sequencing assembly and annotation revealed that the RN12 strain harbored the previously characterized gene clusters for biosynthesis of bacteriochlorophyll (*bch*) and anoxygenic photosynthesis, as well as the gene for leucine/isovalerate utilization (*liu*), encoded in the *A. tertiaricarbonis* strain L108 (3, 11). The average nucleotide identity (ANI) of the common genes between L108 and RN12 was also relatively high. The ANI of *liu* genes and *bchL* (encoding protochlorophyllide reductase subunit) is greater than 85%, corresponding to the arbitrarily recommended cutoff point of 70% DNA-DNA hybridization for bacterial species delineation (12). Therefore, RN12 was identified as a strain of *A. tertiaricarbonis* based on both 16S rRNA gene and chromosomal gene identity. *Aquincola* belongs to

the *Rubrivivax-Roseateles-Leptothrix-Ideonella-Aquabacterium* branch of *Betaproteobacteria* (10). *A. tertiaricarbonis* strain RN12 can form amorphous flocs, similar to those of *Zoogloea resiniphila*, when grown in several other culture media, including *Zoogloea* medium (ZM) and LB broth (Fig. S3). It grew well in the LB broth with no sodium chloride added (salt-free LB) and could also form flocs.

Identification of a large exopolysaccharide biosynthesis gene cluster required for floc formation.The wild-type RN12 strain is resistant to multiple restriction endonucleases, which could be due to the presence of restriction-modification systems. To identify the genes required for floc formation, transposon mutagenesis was conducted on the RN12 strain by using the *mariner* transposon as previously described (9, 13–15). We isolated a series of floc formation-deficient mutants which did not form flocs that could settle to the bottom of culture tubes by gravitational precipitation, and instead the homogenous turbid cell cultures appeared and were composed of single cells when visualized with a microscope (Fig. 1A and B). Most of the transposon insertion has been mapped to a large gene cluster similar to that of *Zoogloea resiniphila* that is required for extracellular polysaccharide biosynthesis (Fig. 1C; Table 1) (9). The cellular role of these genes was further confirmed by genetic complementation analyses in which the plasmid-borne gene could restore the floc-forming phenotype to the specific mutant. It is not surprising that multiple genes encoding glycosyltransferases have been identified to be essential for floc formation. A polysaccharide deacetylase gene was identified in the RN12T40 mutant and a deacetylase was also found to be involved in flocculation (16). These genes, such as glycosyltransferase gene 1 (designated *gt1* here) and the UDP-glucuronate 4-epimerase gene (designated *uge* here), are disrupted in the respective transposon mutants RN12T13 and RN12P20, which are defective in floc formation. Furthermore, the plasmid-borne *gt1* gene (pBBR1MCS-2-*gt1*) and *uge* gene (pBBR1MCS-2-*uge*) restored the floc formation phenotype to these two mutants in genetic complementation analyses (Fig. 2C and E). More importantly, we isolated a series of transposon mutants in which an unexpected *rpoN* gene, encoding the σ^{54} factor, is disrupted (Fig. 1D; Table S1 and Fig. S4).

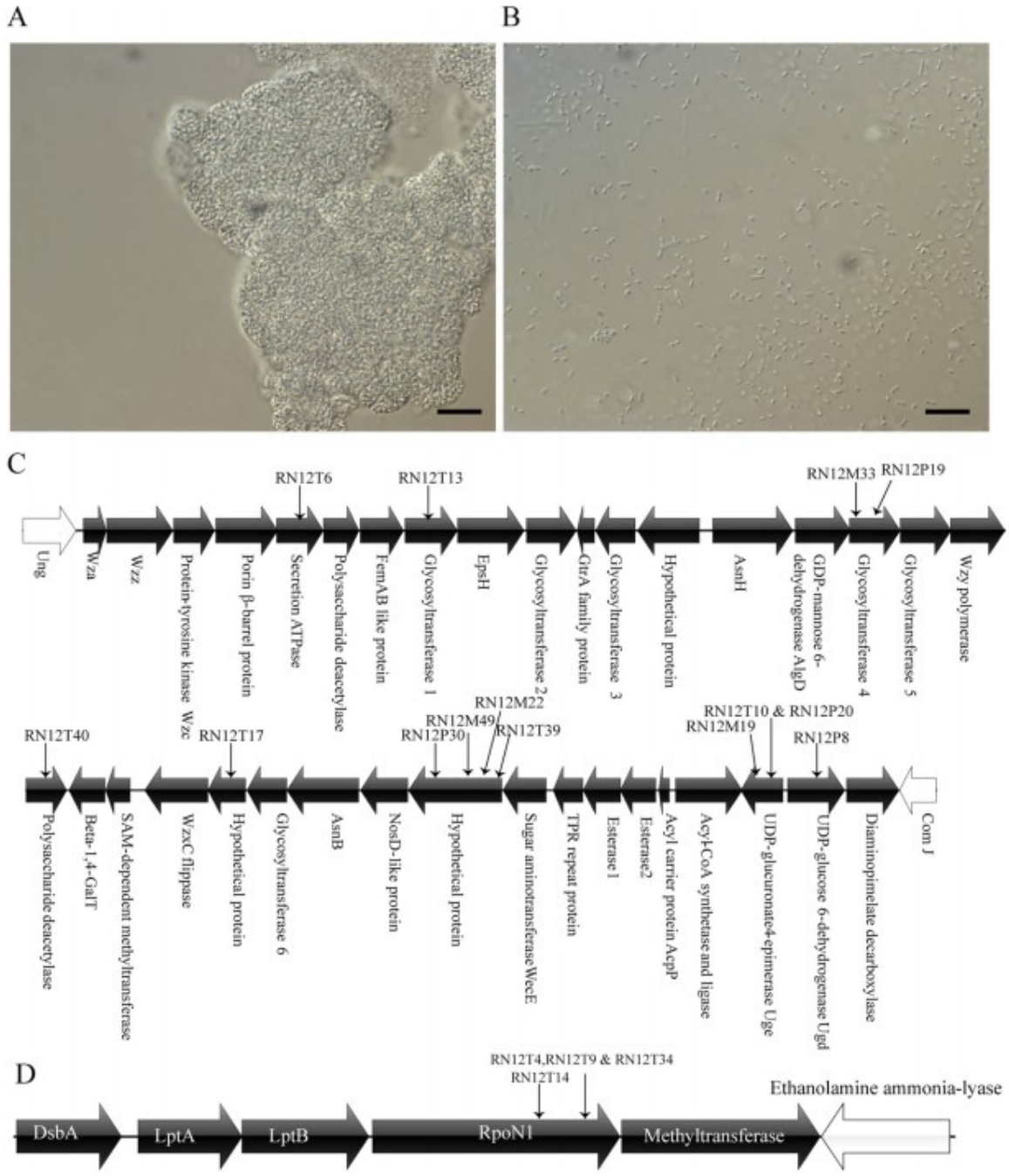

FIGURE 1 Microscopic observations of *Aquincola tertiaricarbonis* RN12 and floc formation-deficient mutants and the mapped transposon insertions. Microphotographs were taken using a light microscope (Nikon Eclipse 80i; Japan) with a DS-Ri1 digital camera (Nikon, Japan), and the image was analyzed using the NIS-Elements D 3.2 program. (A and B) Images of wild-type RN12 (A) and floc formation-deficient mutant RN12T4 (B). Magnification, ×1,000. Bars, 10 μm. (C) The extracellular polysaccharide biosynthesis gene cluster of *A. tertiaricarbonis* RN12 strain and the genes disrupted by insertions of the mariner transposon, mapped in the transposon mutants deficient for bacterial floc formation. (D) Organization of the chromosomal region adjacent to the *rpoN1* gene of *A. tertiaricarbonis* strain RN12 and the gene disrupted by insertions (black arrows) of the mariner transposon, mapped in the transposon mutants deficient for bacterial floc formation.

TABLE 1 Gene products of the extracellular polysaccharide biosynthesis gene cluster of *Aquincola tertiaricarbonis* strain RN12 and the predicted orthologues in the closely related proteobacterial genomes of *Rubrivivax gelatinosus* IL-144 and *Leptothrix cholodnii* SP-6

A. tertiaricarbonis RN12 protein[a]	Predicted function[b]	Polypeptide sequence identity (%) betwen RN12 and[c]:	
		Rubrivivax gelatinosus IL-144	*Leptothrix cholodnii* SP-6
Wza	EPS export	82	62
Wzz	EPS chain length determinant	60	39
Tyrosine kinase Wzc	EPS chain length determinant	69	52
Porin β-barrel	Glycine-rich outer membrane porin for EPS export	32	27
Secretion ATPase	Putative secretion ATPase	72	53
Polysaccharide deacetylase	Removal of acetyl group from EPS	78	—
FemAB-like protein	EPS modification	70	—
Glycosyltransferase 1	EPS unit biosynthesis	63	—
EpsH	Exosortase A	46	27
Glycosyltransferase 2	EPS unit biosynthesis	51	32
GtrA family protein	Unknown	30	—
Glycosyltransferase 3	EPS unit biosynthesis	—	—
Hypothetical protein	Unknown	—	—
AsnH	Asparagine synthesis	71	37
GDP-mannose 6-dehydrogenase AlgD	Production of GDP-mannuronate	35	—
Glycosyltransferase 4	EPS unit biosynthesis	—	—
Glycosyltransferase 5	EPS unit biosynthesis	39	—
Wzy polymerase	EPS polymerase	45	—
Polysaccharide deacetylase	Removal of acetyl group from EPS	36	28
Beta-1,4-GalT	Beta-1,4-galactosyltransferase for EPS unit biosynthesis	—	—
SAM-dependent methyltransferase	SAM-dependent methylation of EPS?	—	—
WzxC flippase	Flipping (export) of EPS units	—	—
Hypothetical protein	Unknown	—	—
Glycosyltransferase 6	EPS unit biosynthesis	37	31
AsnB	Asparagine synthesis	61	—
NosD-like protein	Enzyme maturation protein	52	—
Hypothetical protein	Acetyltransferase (GNAT) for EPS acetylation?		23
Sugar aminotransferase WecE	Production of TDP-4-amino-4,6-dideoxy-D-galactose	—	—
TPR protein	Protein scaffold for EPS synthesis	—	—
Alpha/beta-hydrolase superfamily esterase 1	Modification of EPS?	—	—
Alpha/beta-hydrolase superfamily esterase 2	Modification of EPS?	58	—
Acyl carrier protein AcpP	Lipid and fatty acid metabolism	30	29
Acyl-CoA synthetase and ligase	AMP-dependent synthesis of acyl-CoA	30	—
UDP-glucuronate 4-epimerase Uge	Synthesis of UDP-D-galacturonate	73	67
UDP-glucose 6-dehydrogenase Ugd	Synthesis of UDP-glucuronate	78	74
Diaminopimelate decarboxylase	Unknown	—	—

[a]Proteins shown in boldface are encoded by those genes disrupted by a transposon insertion. SAM, *S*-adenosyl methionine; TPR, tetratricopeptide repeat; CoA, coenzyme A.

[b]EPS, exopolysaccharide.

[c]The NCBI accession number of the reference EPS biosynthesis gene cluster of *Aquincola tertiaricarbonis* RN12 strain is KY053276. —, no orthologue was found.

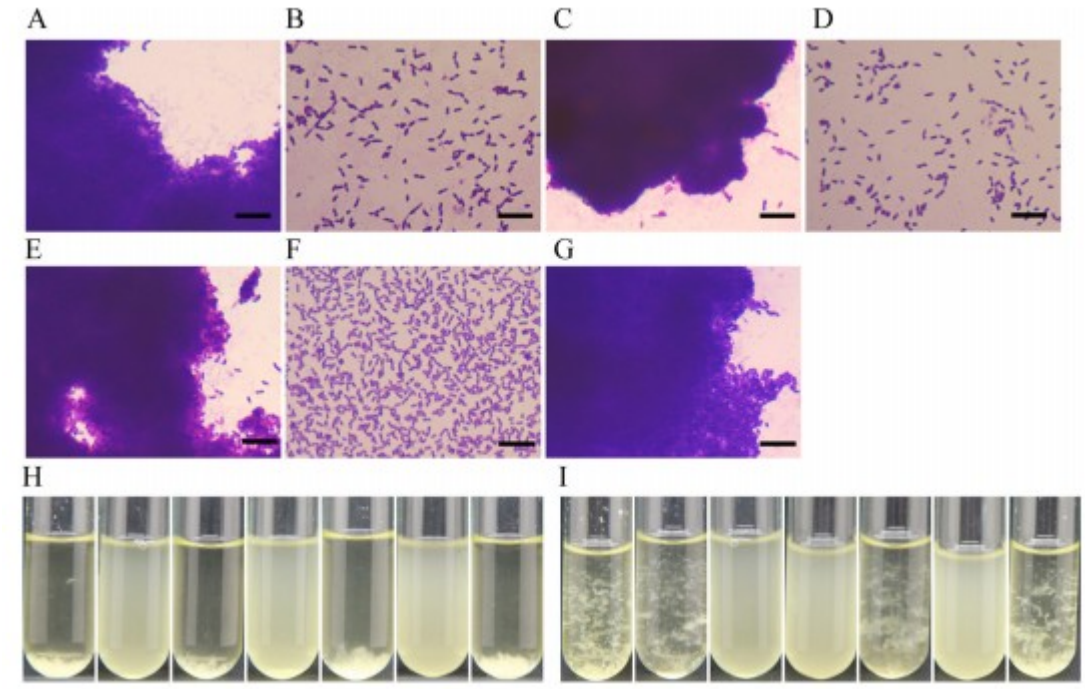

FIGURE 2 The genetic complementation analysis of the glycosyltransferase 1 (*gt1*), UDP-glucuronate 4-epimerase (*uge*), and *rpoN1* in *trans* mutants RN12T13, RN12P20 and RN12T4. Plasmid-borne wild-type *gt1*, *uge*, and *rpoN1* genes restored the phenotype of the RN12T13, RN12P20, and RN12T4 mutants to floc formation, respectively, similar to that of the wild-type strain carrying the empty vector. (A) Wild-type strain with the pBBR1MCS-2 empty vector, visualized under a microscope, after staining with crystal violet solution. (B) RN12T13 mutant with pBBR1MCS-2. (C) RN12T13 mutant with pBBR1MCS-2-*gt1* construct. (D) RN12P20 mutant with pBBR1MCS-2. (E) RN12P20 mutant with pBBR1MCS-2-*uge* construct. (F) RN12T4 mutant with pBBR1MCS-2. (G) RN12T4 mutant with pBBR1MCS-2-*rpoN1* construct. (H) Settled bacterial cultures (cells of bacteria from panels A to G, from left to right). (I) Agitated bacterial cultures (culture tubes contain bacteria from panels A to G, from left to right).

The *rpoN1*-disrupted mutant is deficient for floc formation.

Four of the floc-forming-deficient mutants harbored the transposon in the *rpoN* gene coding for the alternative sigma factor σ^{54} (also called RpoN) in *Escherichia coli* and many other bacteria. The involvement of RpoN in floc formation was further confirmed by genetic complementation analyses. Genome analyses revealed that four RpoN paralogues are encoded in the RN12 genome, and therefore the disrupted *rpoN* paralogues are designated *rpoN1* mutants here. In the *rpoN1*-disrupted mutants (carrying empty vector), bacterial cells could not form the flocs and the homogenous and turbid cultures were similar to those of other non-floc-forming bacteria, such as *Escherichia coli*. Microscopic observation demonstrated that the cells of the *rpoN1* mutants did not aggregate into big flocs and predominately scattered in the culture media. Both the wild-type RN12 strain (carrying empty vector) and the *rpoN1* mutant RN12T4 harboring the complementing pBBR1MCS-2-*rpoN1* construct formed flocs which settled to the culture tube bottom without stirring and shaking (Fig. 2A, F, and G).

Production of released exopolysaccharides in the *rpoN1*-disrupted mutant.

The synthesized polysaccharides were exported out of bacterial cells before the bulk of cells were flocculated by the extracellular polymeric substances, including exopolysaccharides, DNA, and proteins for the formation of bacterial flocs. However, it was revealed that most of the secreted polysaccharides were released and dissolved in the culture broth instead of being bound to and flocculating the bacterial cells when the *rpoN1* gene was inactivated (Fig. 3A and B). Fiber-like materials were precipitated and extracted from the cell-free supernatants of bacterial cultures of the RN12T4 mutant but not other floc-forming or floc-deficient strains of *Aquincola* (Fig. S5A). We figured out a way to estimate the biomass by measuring the wet weight of the spun-down cell pellets, and the results showed that the biomasses of different strains were very close to one another (Fig. S6). Therefore, we extracted and measured the exopolysaccharides of the cell pellets and cell-free supernatants at 12 h, 18 h, and 24 h. In our work, we designated the exopolysaccharides that flocculate the cells as bound exopolysaccharides and the exopolysaccharides that were released and dissolved in the culture broth as soluble exopolysaccharides. We measured the bound exopolysaccharides in the bacterial cell pellets and soluble exopolysaccharides in the supernatants after centrifugation. The soluble exopolysaccharides remained in the supernatants even after ultracentrifugation and could be precipitated by adding ethanol (Fig. S5B). The bound exopolysaccharides decreased for the *rpoN1* mutant by more than 1-fold, while the released exopolysaccharides increased significantly. The plasmid-borne-*rpoN1*-containing mutant had restored amounts of both bound and total exopolysaccharides relative to those of the wild-type strain, thus restoring the floc-forming phenotype (Fig. 3C). It is clear that the disruption of *rpoN1* resulted in the decrease of bound exopolysaccharides and the increase of released exopolysaccharides, which may account for the floc-forming deficiency. Though the biosynthesis of exopolysaccharides remained largely unaffected, those exopolysaccharide chains could not bind to the bulk of cells for the formation of large-sized cell aggregates (flocs). In the absence of RpoN1, the exopolysaccharide chains were readily released into solution and therefore could not play a role in the self-flocculation process of *A. tertiaricarbonis* RN12.

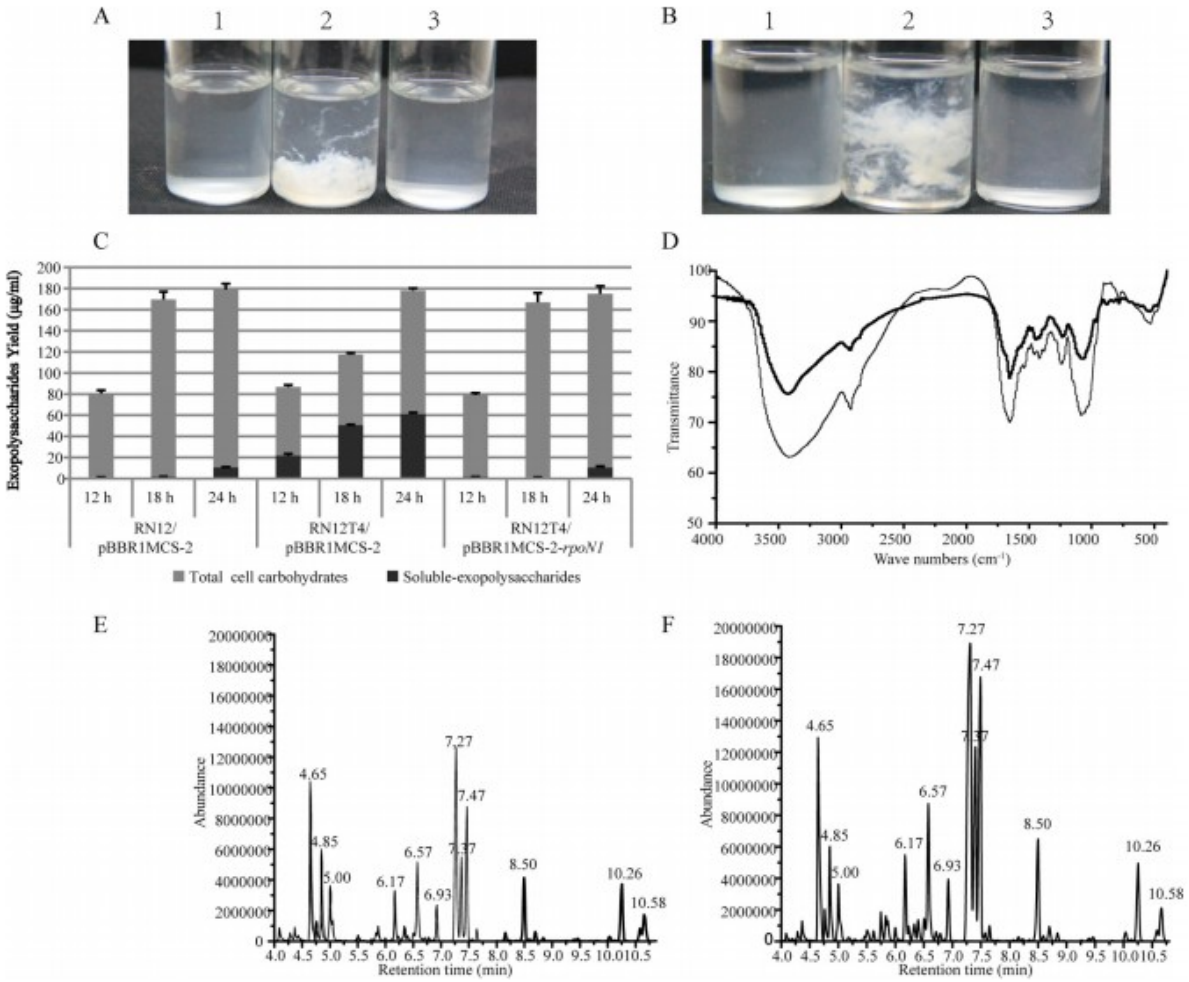

FIGURE 3 Analysis of the extracellular polysaccharides of *A. tertiaricarbonis* of wild-type strain RN12 and *rpoN1* disruptant mutant RN12T4. (A and B) Photographs of settled (A) and agitated (B) exopolysaccharides extracted from the cell-free supernatants of bacterial cultures of the wild-type strain with pBBR1MCS-2, RN12T4 mutant with pBBR1MCS-2, and RN12T4 mutant with pBBR1MCS-2-*rpoN1* construct. (C) Average yields of total cell carbohydrates and released soluble exopolysaccharides were measured using the phenol-sulfuric acid method over the time course of bacterial cultures of *A. tertiaricarbonis*. Values are expressed as micrograms per milliliter of bacterial suspension. All experiments were performed in triplicate; error bars represent standard deviations. (D) Comparison of FT-IR transmittance spectra of bound exopolysaccharides (black line) and soluble exopolysaccharides (gray line). (E and F) Gas chromatogram for TMS methyl glycoside derivatives of hydrolyzed bound exopolysaccharides (E) and soluble exopolysaccharides (F). The peaks at 4.65, 7.27, 7.37, 7.47, 8.50, and 10.26 min (retention times) were identified, using the NIST02 database, as alpha-l-mannopyranoside, alpha-d-galactopyranoside, alpha-d-glucopyranoside, talose, arabinose, and beta-d-glucopyranoside, respectively. The peak at 10.58 min was identified as the internal standard control inositol. The bound exopolysaccharides were extracted from the cell pellets of *A. tertiaricarbonis* RN12 and the released soluble exopolysaccharides were extracted from the supernatant of the floc formation-deficient mutant RN12T4 cultures.

The exopolysaccharides of the wild-type strain and mutants were extracted and analyzed qualitatively and quantitatively. We found that exopolysaccharides could hardly be separated from the bacterial flocs of the wild-type strain by using the activated sludge exopolysaccharide extraction procedure previously described (17), and most of the bacterial flocs

remained almost intact after the multiple-step extraction of exopolysaccharides (Fig. S7). We directly measured the polysaccharide quantities of cell pellets before and after the polysaccharide extraction. Most of the exopolysaccharides remained in those intact bacterial flocs after the extraction of exopolysaccharides, and the bound exopolysaccharides were remarkably underestimated by this approach (Fig. S8). Therefore, we developed a new method to estimate the bound exopolysaccharides. The cell pellets of different strains were directly treated with sulfuric acid, and the carbohydrates were hydrolyzed and oxidized. The total cell carbohydrates were measured by the phenol-sulfuric acid method to determine exopolysaccharides (Fig. 3C). These results suggest that the exopolysaccharides were extremely tightly bound to the bulk of bacterial cells in the flocs via a yet-unknown mechanism.

The bound and released exopolysaccharides are highly similar in monosaccharide composition.

The monosaccharide compositions of exopolysaccharides extracted from the *A. tertiaricarbonis* strains were analyzed using gas chromatograph-mass spectrometry (GC-MS). The analyses revealed the presence of hexoses (12.36% mannopyranoside, 17.29% galactopyranoside, 11.20% glucopyranoside, and 9.50% talose) and pentoses (5.16% arabinose) in the exopolysaccharides. The peaks at 4.65, 7.27, 7.37, 7.47, 8.50, and 10.26 min (retention times) were identified by the NIST02 database as alpha-L-mannopyranoside, alpha-D-galactopyranoside, alpha-D-glucopyranoside, talose, arabinose, and beta-D-glucopyranoside, respectively (Fig. 3E and F). The chemical structures of the bound exopolysaccharides and soluble exopolysaccharides extracted from the cell pellets of wild-type strain RN12 and the cultivation supernatant of the *rpoN1* mutant were compared to reveal whether the increase of released exopolysaccharides of the *rpoN1* mutant actually came from the originally bound exopolysaccharides of the wild-type strain. In a Fourier transform infrared spectroscopy (FT-IR) analysis, the positions and numbers of FT-IR peaks of the two types of exopolysaccharides appeared to be highly similar (Fig. 3D), suggesting that their chemical groups and structures are similar. More importantly, the major and credible peaks of these two exopolysaccharides were highly similar in the GC-MS analyses. Therefore, both FT-IR and GC-MS results showed that the bound and soluble exopolysaccharides are highly similar. In addition, the FT-IR spectra of the two types of exopolysaccharides showed a broad stretching vibration of N-H and O-H (3,500 to 3,100 cm^{-1}) and a weak C-H stretching peak of a methyl group at 2,926 cm^{-1}. Infrared bands at 1,652.2 cm^{-1} (amide I) and 1,544.7 cm^{-1} (amide II) were attributed to the amide bond of the *N*-acetyl groups.

The exopolysaccharide biosynthesis genes are not regulated by RpoN.

Disruption of the *rpoN1* mutant resulted in a bacterial deficiency in floc formation. However, reverse transcription-PCR (RT-PCR) and real-time PCR

analyses demonstrated that the transcription levels of two exopolysaccharide biosynthesis genes were comparable in the wild-type and the *rpoN1* mutant (Fig. 4A, B, and C), indicating that this exopolysaccharide biosynthesis gene cluster might not be regulated by the RpoN1 sigma factor. These results are also consistent with our finding that the biosynthesis of exopolysaccharides remained largely unaffected in the *rpoN1* disrupted mutant. However, the bound exopolysaccharides formed in the wild-type strain were released into the culture broth as soluble exopolysaccharides, which might no longer be able to flocculate the cells to form cell aggregates/flocs in the absence of certain proteins whose genes are transcriptionally regulated by RpoN1. Furthermore, the transcriptional start site mapping of *uge* determined by primer extension analysis revealed the conserved −35 (CGGTCC) and −10 (TAACGT) promoter motifs. There were no typical −24 (GG) and −12 (GC) motifs upstream of the transcriptional start site C (+1), and thus the *uge* gene and downstream genes may not be regulated by σ^{54} factor RpoN (Fig. S9).

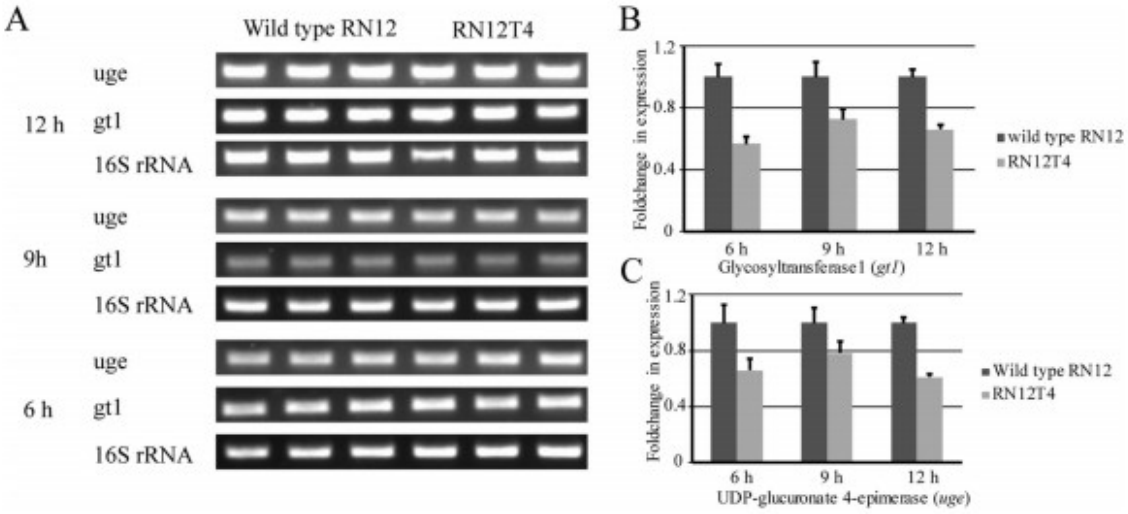

FIGURE 4 Expression of glycosyltransferase 1 (*gt1*) and UDP-glucuronate 4-epimerase (*uge*) genes in wild-type RN12 and the *rpoN1*-disrupted mutant RN12T4. Bacteria were cultivated at 28°C in the R2A medium with shaking (220 rpm). (A) Transcription of the *gt1* and *uge* genes was examined by using semiquantitative RT-PCR and real-time PCR. 16S rRNA gene expression was analyzed and used as the loading control. (B and C) Transcription of the *gt1* (B) and *uge* (C) genes was examined by real-time PCR. Relative expression levels were calculated according to the $2^{-\Delta\Delta CT}$ method (72), with the 16S rRNA gene as an internal control and the wild-type RN12 as a calibrator (relative expression set to 1). The assays were performed in triplicate; error bars represent the standard deviations.

Cell surface hydrophobicity of the *rpoN1* mutant was higher.

We tested the hydrophobicity of the cell surfaces of the wild-type strain and *rpoN1* mutant over the 36-h incubation period. The results showed that the cell surface hydrophobicity of the wild-type strain (14.91% to 26.71%) was dramatically lower than that of the *rpoN1* mutant (56.96% to 84.45%) (Table S2). These results indicated that the cell surface of the *rpoN1* mutant might carry much lower levels of hydrophilic substances, such as

exopolysaccharides, which could dramatically decrease the cell surface hydrophobicity (18, 19).

Disruption of *rpoN1* affects biofilm formation and swarming ability.

RpoN regulates a series of cellular functions, including cell motility and biofilm formation (20–23). To confirm whether RpoN1 regulates swarming motility in *A. tertiaricarbonis* RN12, as previously revealed for many other bacteria, the swarming motility test was performed on semisolid R2A agar plates containing 0.4% (wt/vol) agar which we inoculated with a 5-μl drop of bacterial culture. We found that the *rpoN1* insertion mutant was defective in swarming motility and that this defect was fully restored by expression of *rpoN1* in *trans* (Fig. 5A and B). The genetic complementation analyses indicated that the *rpoN1* gene was required for swarming motility. In addition, inactivation of *rpoN1* resulted in the downregulation of type IV prepilin gene *tapA* in the RN12T4 mutant compared to the wild-type strain (Fig. 6A, B, and C), which may partly account for the decrease of swarming motility in this mutant (24–27). Furthermore, the transcriptional start site mapping of *tapA* was determined by primer extension analysis and revealed that the conserved −24/−12 motifs (GG and GC) characteristic of σ^{54}-dependent promoters were present upstream of the open reading frame (Fig. 6D). On the other hand, overexpression of a pBBR1MCS-2-borne *tapA* gene in *trans*, driven by the housekeeping sigma factor RpoD-dependent P*lac* promoter, did not restore the floc-forming phenotype to the RN12T4 mutant, indicating that pilin may not be involved in floc formation (Fig. S10).

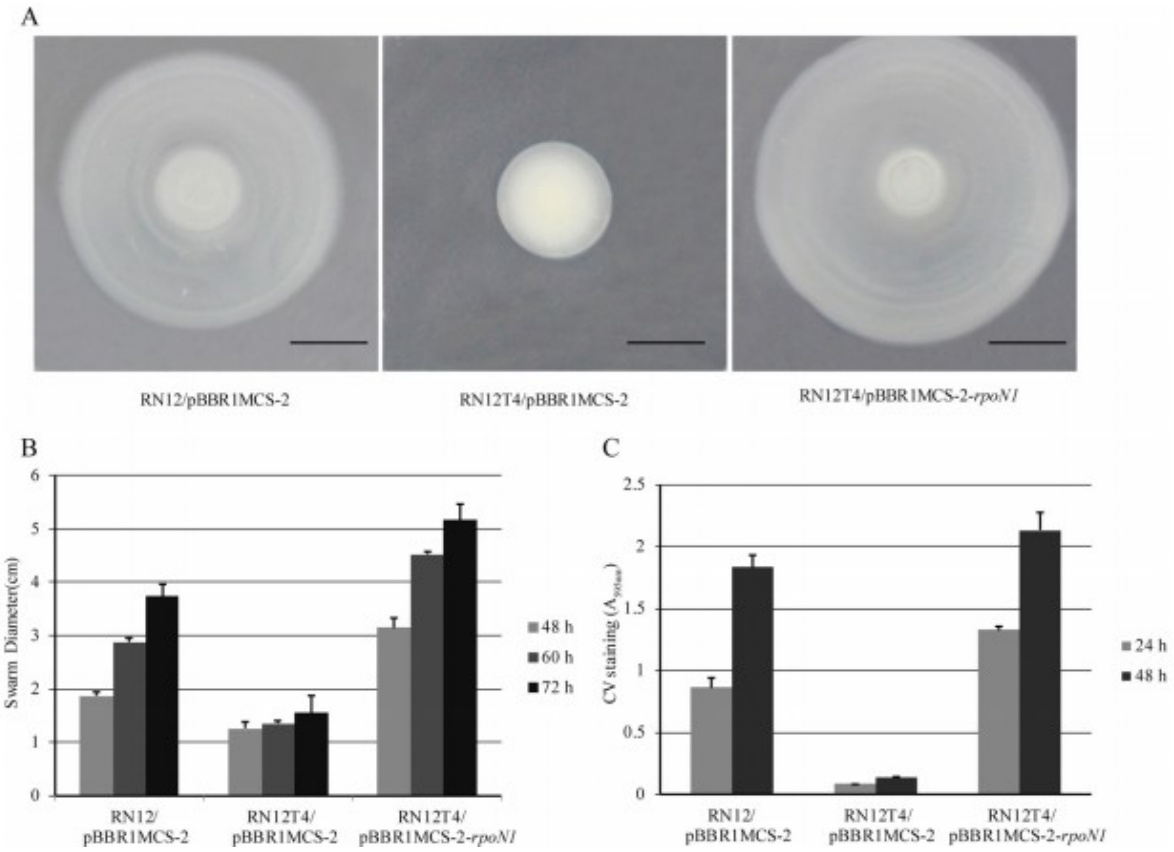

FIGURE 5 Genetic complementation analysis of the swarming motility and biofilm formation of *rpoN1* disruptant mutants of *A. tertiaricarbonis*. (A) Colony morphology of each strain after a 3-day incubation. Bar, 1 cm. (B) Swarming motility, expressed as colony diameters at 48 h, 60 h, and 72 h. (C) Biofilm levels measured after 24 h or 48 h of incubation at 28°C in the R2A medium. Each sample was plated in quadruplicate. Biofilms were stained with 0.1% crystal violet (CV). Crystal violet was dissolved in 30% acetic acid. Biofilms were quantified by measuring the optical density at 595 nm. Error bars represent the standard deviations.

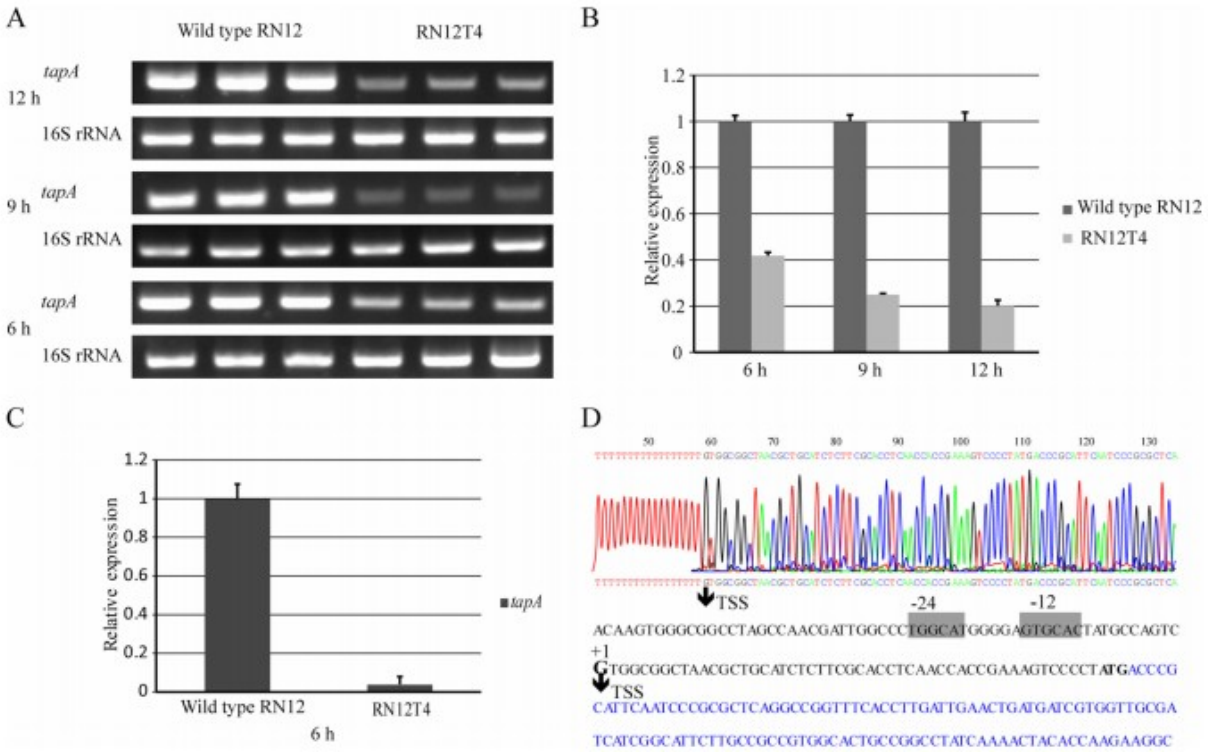

FIGURE 6 Transcription of the prepilin gene *tapA* over the time course in the wild-type strain of *A. tertiaricarbonis* RN12 and the *rpoN1*-disrupted mutant RN12T4. Bacteria were cultivated at 28°C in the R2A broth with shaking (220 rpm), The data shown represent samples collected at 6 h, 9 h, and 12 h. (A) Transcription of the *tapA* gene was examined by using semiquantitative RT-PCR. 16S rRNA gene expression was analyzed and used as the loading control (71). (B) Trace quantity plotting of data from panel A, using Quantity One software. The assays were performed in triplicate. (C) Transcription of the gene was examined by real-time PCR. Relative expression levels were calculated according to the $2^{-\Delta\Delta CT}$ method (72), with the 16S rRNA gene as an internal control gene and the wild-type RN12 as a calibrator (relative expression set to 1). The assays were performed in triplicate. Error bars represent the standard deviations. (D) Determination of the transcriptional start site (TSS) of the type IV prepilin gene tapA in A. tertiaricarbonis strain RN12. The blue sequence is the open reading frame of tapA, and the nucleotide G with an arrow connected underneath it represents the determined transcriptional start site (+1). The shadowed sequences TGGCAT and GTGCAC are the putative −24 and −12 motifs of the promoter putatively recognized by the sigma factor RpoN1.

Biofilm formation was evaluated in liquid R2A medium without agitation in 96-well plates for 2 days as previously described (28, 29). The biofilm formation decreased in the *rpoN1* mutant RN12T4 (carrying empty vector) compared to that of the wild-type RN12 (carrying empty vector) and the *rpoN1* mutant harboring the complementing pBBR1MCS-2-*rpoN1* construct (Fig. 5C). This result showed that RpoN1 upregulates biofilm formation in *A. tertiaricarbonis* RN12. These results also indicated that RpoN1 functions similarly in this bacterium as its orthologues do in *Vibrio fischeri* and other well-studied bacteria (20, 22, 30). It was revealed that the *rpoN1* mutant was deficient in floc formation and lack of biofilm formation at the air-liquid interphase (Fig. S11).

Functions of four *rpoN* genes in *A. tertiaricarbonis* strain RN12.

Interestingly, genome sequencing and annotation revealed that four *rpoN* paralogues were present in the *A. tertiaricarbonis* RN12, as mentioned above, though only one RpoN was encoded in most of the sequenced bacteria. It has also been revealed that some bacteria, including *Xanthomonas oryzae* pv*. oryzae*, *Bradyrhizobium japonicum*, *Rhizobium etli*, *Burkholderia fungorum*, and *Ralstonia solanacearum*, carry two copies of *rpoN* (31–34), and four copies of *rpoN* are encoded in the genome of *Rhodobacter sphaeroides* (35). The four paralogues were designated *rpoN1*, *rpoN2*, *rpoN3*, and *rpoN4*, and their G+C contents were 68.29%, 68.48%, 69.57%, and 56.13%, respectively. The lower G+C contents indicated that *rpoN4* might have been recently acquired via horizontal gene transfer. A molecular phylogenetic tree was constructed based on the polypeptide sequences. Phylogenetic analyses showed that RpoN1 might be orthologous to the RpoN homologue of the closely related strains *Rubrivivax gelatiinosus* IL-144 and *Methylibium petroleiphilum* PM1 (Fig. S2B). It is evident that these four RpoN proteins contain the conserved regions characteristic of the σ^{54} factors (Fig. S12), with the exception of region II, which is known to be variable and almost absent in the RpoN protein from *R. capsulatus* and *R. sphaeroides* (36–39). The RpoN regions that bind the −12 and −24 promoter elements are a helix-turn-helix (HTH) motif and a highly conserved region named the RpoN box, respectively (40). The RpoN box (corresponding to residues 453 to 463 of the *E. coli* RpoN) is highly conserved in the four RpoN paralogues from *A. tertiaricarbonis* RN12, and more importantly, the HTH motif (residues 366 to 386 of *E. coli* RpoN) is also well conserved. The *rpoN2*, *rpoN3*, and *rpoN4* genes were cloned into the shuttle vector pBBR1MCS-2, and the resultant constructs were transferred into the RN12T4 mutant via conjugation. However, the overexpression of the *rpoN2*, *rpoN3*, and *rpoN4* paralogues failed to restore the floc-forming phenotype to RN12T4, as shown with the *rpoN1* genetic complementation analyses (Fig. S13). Expression of *rpoN2* in *trans* did enhance the swarming motility of the *rpoN1* mutant RN12T4, and two other *rpoN* paralogues could somehow complement the RpoN1-regulated swarming capability (Fig. S14). However, the overexpression of the *rpoN2*, *rpoN3*, and *rpoN4* paralogues could not restore the biofilm formation phenotype to RN12T4, as shown in the *rpoN1* genetic complementation analyses (Fig. S11). These results indicate that these four *rpoN* paralogues are not functionally interchangeable, and the *rpoN1* paralogue plays a major role in the transcriptional regulation of the downstream *tapA* pilin gene and other unidentified genes involved in floc formation and swarming motility.

DISCUSSION

In this study, we demonstrated that a large exopolysaccharide biosynthesis gene cluster and a regulatory gene, *rpoN1*, are required for the floc-forming phenotype in *A. tertiaricarbonis* strain RN12. The genes of this gene cluster are involved in biosynthesis, modification, and secretion of exopolysaccharides. Previously, we also identified a similar gene cluster

required for floc formation of the activated sludge bacterium *Zoogloea resiniphila* MMB (9). Notably, the two asparagine synthetase genes *asnB* and *asnH* are also present in the exopolysaccharide biosynthesis gene cluster of *A. tertiaricarbonis* RN12, and an *asnB*-disrupted transposon mutant has been isolated and exhibits a floc-forming deficiency as previously shown with *Zoogloea* (data not shown). The involvement of *asnB* in floc formation, however, has not been confirmed by genetic complementation in *A. tertiaricarbonis* RN12 strain. More importantly, transposon insertion has been repeatedly mapped to the *rpoN1* gene coding for the alternative sigma factor RpoN (σ^{54}) in the floc formation-deficient mutants, and a total of four *rpoN* paralogues have been found in the genome of strain RN12. Their cellular functions in the regulation of biofilm formation, swarming motility, and floc formation had been preliminarily investigated by comparing the phenotypic changes of the RN12T4 mutant, in which the plasmid-borne *rpoN* paralogues were expressed in *trans*. It is well known that the RpoN sigma factor is an important transcriptional regulator for bacterial responses to environmental stresses, including swarming motility and biofilm formation in many bacterial species (20–23, 41). Our studies also verified the key role of RpoN1 in swarming motility and biofilm formation in *A. tertiaricarbonis* strain RN12. More research is needed to investigate the cellular roles of RpoN paralogues in the *A. tertiaricarbonis* RN12 strain.

Extracellular polysaccharides act as matrix materials and are essential for formation of biofilms in most Gram-negative bacteria (42–44). Our study also demonstrated that biosynthesis and secretion of extracellular polysaccharides play very important roles in the formation of bacterial flocs, in which bulks of bacterial cells are flocculated by a self-secreted common gelatinous matrix. Bacterial flocs, suspended in ambient water, represent the third form of bacterial growth and survival, in addition to two well-documented forms, planktonic single cells and multicellular biofilms attached to biological and nonbiological surfaces. The dramatic changes in the bacterial gene expression, morphology, and physiology under the two growth states of planktonic cells and biofilms have been well characterized (43, 45–48). Bacterial biofilm formation is controlled and coordinated by a series of cellular signaling pathways (43, 44, 49, 50). Bacterial floc formation has played a crucial role in the widely utilized activated sludge process for sewage and wastewater treatment for over 100 years. On the other hand, such bacterial flocs formed by iron-oxidizing bacteria, such as filamentous *Leptothrix* strains, also cause problems in drinking water wells and water supply pipelines (2). It remains unknown how and whether the *A. tertiaricarbonis* RN12 strain plays a critical role in the formation of brown flocculent precipitates in the well and tap water of Xishui County.

The biosynthesis and secretion of the extracellular polysaccharides most likely resemble those of lipopolysaccharide (O antigen). Compared to non-floc-forming bacteria, further modification or processing of extracellular polysaccharides may also be necessary for the organization and assembly of

the gelatinous matrix required for floc formation in *Aquincola*, *Zoogloea*, and other floc-forming bacteria. The modification and processing of exopolysaccharides might be mediated by the RpoN1-dependent transcription of a certain gene(s), since the biosynthesis and secretion of exopolysaccharides remained unaffected or even increased in *rpoN1*-disrupted mutants, in which the bacterial flocs were not formed and instead bacterial single cells grew in the planktonic state. Most of the exopolysaccharides synthesized in the *rpoN*-disrupted mutants were released as the soluble exopolysaccharides dissolved in the liquid broth. Consistent with this, the transcription of two exopolysaccharide biosynthesis genes was only moderately affected by the disruption of *rpoN1* (Fig. 4). However, the polysaccharide chains were not tightly bound to the cells or cell aggregates; the mechanism by which this tight binding occurs is currently unknown. The bound exopolysaccharides might be required for floc formation by holding the bacterial cells together. Taken together, our results indicate that RpoN1 might regulate the expression of certain genes involved in the self-flocculation of bacterial cell aggregates other than the biosynthesis and secretion of extracellular polysaccharides required for floc formation. Our efforts to establish in-frame deletion in this *Aquincola* strain have not yet been successful, limiting the more-in-depth investigation into the mechanism underlying floc formation which may involve both exopolysaccharides and other secreted biopolymers. The yet-unidentified factor(s) obviously plays an important role in the formation of the tightly bound exopolysaccharides and bacterial flocs. Further investigation is required to reveal the mechanisms underlying floc formation and its cellular functions in bacteria.

MATERIALS AND METHODS

Bacterial strains, plasmids, and culture conditions.

The bacterial strains and plasmids used in this study are listed in Table 2. Bacterial strains were cultured in the Luria-Bertani (LB) broth (5 g/liter yeast extract, 10 g/liter tryptone, 10 g/liter NaCl; pH 7.0) or plates, R2A medium (supplemented with 15 μg/ml of gentamicin or 50 μg/ml of kanamycin and 50 μg/ml of diaminopimelic acid, when necessary) (51), and *Zoogloea* medium (ZM) (52). The *A. tertiaricarbonis* RN12 strains were grown at 28°C in R2A medium and salt-free LB broth.

TABLE 2 Bacterial strains and plasmids used in this study

Strain or plasmid	Description[a]	Reference or source
E. coli strains		
DH5α	F⁻ *endA1 glnV44 thi-1 recA1 relA1 gyrA96 deoR nupG ϕ80dlacZΔ*M15 Δ(*lacZYA-argF*)*U169 hsdR17*(r_K^- m_K^-) *phoA* λ^-	Novagen
WM3064	*thrB1004 pro thi rpsL hsdS lacZ*ΔM15 *RP4-1360* Δ(*araBAD*)*567 dapA1341*::[*erm pir*]	W. Metcalf
A. tertiaricarbonis strains		
RN12	Floc-forming strain	This study
RN12T4 mutant	*mariner* transposon insertion in *rpoN1* at nt 1274	This study
RN12T13 mutant	*mariner* transposon insertion in *gt1* at nt 710	This study
RN12P20 mutant	*mariner* transposon insertion in *uge* at nt105	This study
Plasmids		
pFAC	*mariner* transposon delivery plasmid R6K, Gm^r	13
pminiHmarRB1	*mariner* transposon delivery plasmid R6K, Km^r	58
pBBR1MCS-2	Broad-host-range shuttle vector	59
pBBR1MCS2-*rpoN1*	*rpoN1* gene cloned in pBBR1MCS-2, Km^r	This study
pBBR1MCS2-*rpoN2*	*rpoN2* gene cloned in pBBR1MCS-2, Km^r	This study
pBBR1MCS2-*rpoN3*	*rpoN3* gene cloned in pBBR1MCS-2, Km^r	This study
pBBR1MCS2-*rpoN4*	*rpoN4* gene cloned in pBBR1MCS-2, Km^r	This study
pBBR1MCS2-*gt1*	*gt1* gene cloned in pBBR1MCS-2, Km^r	This study
pBBR1MCS2-*uge*	*uge* gene cloned in pBBR1MCS-2, Km^r	This study

[a]Gm^r, gentamicin resistance; Km^r, kanamycin resistance.

Bioinformatics tools and genome sequencing and annotation.

The DNA sequencing, assembly, and annotation of the bacterial genome were conducted by using the Illumina Miseq sequencing platform, the SOAP *de novo* version 2.21 package, and the RAST (Rapid Annotation using Subsystems Technology) server (53, 54), respectively. Nucleotide and protein sequences were retrieved from the NCBI database at the National Center for Biotechnology Information by using BLAST searches (http://www.ncbi.nlm.nih.gov/BLAST). Multiple sequence alignments were performed by using the Clustal X alignment program (55) and GENEDOC software (56). The phylogenetic trees of the 16S RNA gene and other genes were generated using the neighbor-joining (NJ) method and MEGA version 6.0 software (57).

Transposon mutagenesis and genetic complementation.

The *mariner* transposon mutant libraries were generated as previously described (13, 58) and screened by observing the floc-forming deficiency in R2A broth. *Escherichia coli* WM3064 strains carrying the transposon delivery suicide plasmids pmini*Hmar* RB1 (courtesy of Daad Saffarini) and pFAC (courtesy of John Mekalanos) as the donor strain and the *A. tertiaricarbonis* RN12 strain as the recipient strain for biparental conjugation. After 4 to 6 h of mating on LB agar plates supplemented with diaminopimelic acid, the bacterial cells were diluted and plated on R2A agar plates supplemented with gentamicin (15 μg/ml) and kanamycin (50 μg/ml). The single colonies were inoculated into each well of the 96-well plates, 200 μl of fresh R2A medium

was added, and floc formation was observed. The mutants deficient in floc formation were subjected to further analyses. The transposon insertion site in each mutant was mapped as previously described (14). The chromosomal DNAs of these strains were digested with PstI and ligated to generate circular closed DNA molecules by using T4 DNA ligase (TaKaRa, Dalian, China). The circular closed DNA was then used as the template for inverse PCR. For genetic complementation analyses, the target genes were PCR amplified and cloned into the pBBR1MCS-2 vector (59). The resultant constructs and empty vector were transferred into the *A. tertiaricarbonis* RN12 wild-type strain and mutant strains via conjugation, using WM3064 as a donor strain. The primers used are listed in Table 3.

TABLE 3 Primers used in this study

Primer use and name	Sequence (5′–3′)	Restriction site
Complementation primers		
rpoN1F	5′-CGGAATTCATGAAACCCTCGCTGCAAATCCG-3′	EcoRI at 5′ end
rpoN1R	5′-GCTCTAGAGCAGGAACAGGGCAATCTGGGGC-3′	XbaI at 5′ end
rpoN2F	5′-GGAATTCACACTGTTTCTAACGCCTACC-3′	EcoRI at 5′ end
rpoN2R	5′-GCTCTAGACGACGAGTTCTAGGGTTTCAG-3′	XbaI at 5′ end
rpoN3F	5′-GGAATTCCGGAGTACCTTGTCCCATG-3′	EcoRI at 5′ end
rpoN3R	5′-GCTCTAGATTCAACCACCACAAGGAGC-3′	XbaI at 5′ end
rpoN4F	5′-GGAATTCGCGCACATCACACCTGAAGAG-3′	EcoRI at 5′ end
rpoN4R	5′-GCTCTAGAATAAGGGCCTGACTAAGCGAC	XbaI at 5′ end
gt1-F	5′-GGAATTCAACCCCAGCAACGCCAAGTA-3′	EcoRI at 5′ end
gt1-R	5′-GCTCTAGAAGGAAGGCATGGGTGAAGG-3′	XbaI at 5′ end
uge-F	5′-CGGAATTCTGCCCACTCCATCATGAAAAT-3′	EcoRI at 5′ end
uge-R	5′-GCTCTAGACGATCAGACCTTGTAGTAGCC-3′	XbaI at 5′ end
Real-time PCR primers		
Q-gt1-F	5′-GCGGTGATCGTGTTCTCGTC-3′	
Q-gt1-R	5′-GGCGTATTCGGTCCACTTGG-3′	
Q-uge-F	5′-CCGACAACCTCAACGCCTACT-3′	
Q-uge-R	5′-CATCTGCTGGAAGCGGAAAC-3′	
Q-Tap F	5′-AGTTCACGGAGGTCGTTTCG-3′	
Q-Tap R	5′-AGCAATCACGCCTTGGGTAG-3′	
Q-16S-F	5′-CGTGTAGCAGTGAAATGCGTAG-3′	
Q-16S-R	5′-GAAACCCTCCCAACAACCAG-3′	
RT-PCR primers		
RT-TapA-F	5′-CTACACCAAGAAGGCGAAGT-3′	
RT-TapA-R	5′-AGGAGCAGGTGCCCGATT-3′	
RT-16S-F	5′-CTGAGAGGACGACCAGCCACAC-3′	
RT-16S-R	5′ -TACGCATTTCACTGCTACACGC-3′	
Primer extension primers		
tapA-SP1	5′-GCCGTCGGAGTAATAATGTA-3′	
tapA-SP2	5′-CGTTAGCGATTGCGATAGA-3′	
uge-SP1	5′-CTCGGAAAACGGCATCT-3′	
uge-SP2	5′-GAGCTGGAGGCATACAC-3′	
oligo(dT)	5′-GCCAGTCTTTTTTTTTTTTTTTT-3′	

Exopolysaccharide extraction, purification, and quantification.

Exopolysaccharide extraction was conducted as previously described with modification (60, 61). Wild-type and mutant strains were grown at 28°C in R2A broth with shaking (220 rpm). Exopolysaccharides of the wild-type strain and mutants were isolated from both cell pellets and culture supernatants. The bacterial cell pellets were collected after centrifugation at 10,000 ×*g* for

30 min, and the released crude exopolysaccharides were precipitated by addition of 3 volumes of ice-cold 95% (vol/vol) ethanol to the supernatants. Cell pellets of the wild type were suspended in 100 ml of 0.14 M sodium chloride and vigorously shaken for 1 h to separate the exopolysaccharides from cell surfaces. The supernatants were also collected after centrifugation at 10,000 ×*g* for 30 min. After 1 h of incubation in the ice bath, the precipitates were collected and washed twice using 95% (vol/vol) ethanol and one more time with absolute ethanol. The precipitates were resuspended in 50 mM Tris-HCl buffer (pH 7.5) containing 10 mM $MgCl_2$ and then digested with DNase I (10 μg/ml; Sigma) and RNase A (10 μg/ml; Sigma) at 37°C for 12 h and treated with proteinase K (100 μg/ml) at 37°C overnight. The exopolysaccharide samples were precipitated with ethanol as described above and dried by freeze-drying. The carbohydrate contents of each exopolysaccharide extract and cell pellet were measured by the phenol-sulfuric acid method using D-glucose as a standard (62). Concentrations of exopolysaccharide are expressed as micrograms per milliliter of bacterial culture.

FT-IR spectroscopy.

The exopolysaccharide samples were analyzed using a Nicolet 5700 FTIR spectrometer (Thermo Fisher, USA). The scanning conditions were as follows: a spectral range of 4,000 to 400 cm, 64 scans, and a resolution of 4 cm^{-1} to 0.09 cm^{-1} (63).

TMS derivatizaion and GC-MS analysis.

The exopolysaccharide samples were subjected to GC-MS using BSTFA [*N*,*O*-bis(trimethylsilyl) trifluoroacetamide] derivatization to generate per-*O*-trimethylsilyl (TMS) methyl glycosides (64, 65). One microliter of *myo*-inositol solution (1 mg ml^{-1}) was added to 1 mg of dried exopolysaccharide samples and then lyophilized to dryness (66). The dried samples were hydrolyzed with 500 μl of methanolic-HCl (1 M) for 16 to 18 h at 80°C. After hydrolysis, samples were dried under N_2, and 100 μl of methanol was added to remove residual acid and dried by N_2 gas flushing for a total of three times. Next, 200 μl of methanol-pyridine-acetic anhydride (4:1:1) solution was added to N-acetylate the samples, and mixtures were incubated at 100°C for 1 h. The samples were dried under N_2 and derivatized by adding 200 μl of BSTFA and incubated at 80°C for 30 min. Samples were dried and resuspended in 500 μl hexane and analyzed by GC-MS. One microgram of inositol was added to each tube as an internal standard, and D-glucose and starch were used as positive and negative controls, respectively.

Biofilm and swarming motility assay.

Relative biofilm production levels were assayed using the 96-well crystal violet staining method as described previously (28, 29). Bacterial cultures were grown overnight in R2A broth and diluted by 20-fold steps with fresh broth. Aliquots of 100 μl of the diluted cultures were placed into the 96-well

plates. Each sample was plated in quadruplicate, and the wild-type strain was used as a control for each plate. The duplicate plates were grown at 28°C for 24 h and 48 h, respectively. The crystal violet staining was conducted as previously described, and the formation of biofilm was monitored by measuring the optical density at 595 nm via a Thermomax spectrophotometer.

Swarming motility was assayed using soft R2A agar medium with 0.4% agar, following the procedure as previously described (67, 68). The bacterial strains were grown overnight in R2A broth, and 5 µl of the culture was plated on an individual petri dish in triplicates. Motility was visualized as a white halo of cells moving outward from the original inoculation site after 3 days of incubation at 28°C. The diameters of the colonies were measured and photographed.

Cell surface hydrophobicity test.

The bacterial adhesion to hydrocarbon (BATH) assay was used to measure the cell surface hydrophobicity (69, 70). The bacterial cultures were centrifuged at 5,000 ×*g* for 10 min. Cells were washed once with MSM medium (2.0 g Na_2HPO_4, 0.75 g KH_2PO_4, 0.5 g $MgSO_4 \cdot 7H_2O$, 1.0 g NH_4Cl per liter; adjusted to pH 7.0) and resuspended to an optical density of 0.4 measured at 600 nm by using a Thermomax spectrophotometer. Four milliliters of the cell suspension was added to the 15-ml test tube with 1 ml dodecane and mixed on a vortex mixer at full speed for 2 min. The mixture was allowed to separate for 15 min at room temperature, and the lower aqueous phase was carefully removed. The hydrophobicity was calculated by comparing the optical density of the aqueous phase before and after the treatment.

RNA extraction, real-time PCR, and RT-PCR analysis of gene transcription.

Total RNA was extracted by using RNAiso Plus (TaKaRa) and an RNAprep pure cell/bacteria kit (Tiangen Biotech, Ltd., Beijing, China). RNA was further purified using a DNase I treatment. The integrity of RNA was evaluated by agarose (0.8%) gel electrophoresis. The concentration and purity of RNA were measured on a spectrophotometer (Nanodrop Technologies, Wilmington, DE, USA). To prepare cDNA, 2 µg of total RNA was reverse transcribed using the PrimeScript RT reagent kit with gDNA eraser (TaKaRa) and TIANscript RT kit (Tiangen Biotech, Beijing, China) according to the manufacturer's protocol. Semiquantitative PCR analyses were carried out as described previously (71). Quantitative real-time PCR was performed using 1 µl of 10-fold-diluted cDNA in 20 µl total volume. The relative gene expression levels were quantified using SYBR Premix DimerEraser (TaKaRa) on a Roche LightCycler 480 II real-time PCR system (Roche Diagnostics, Penzberg, Germany). Cycling conditions were as follows: 30 s at 95°C, followed by 40 cycles each consisting of 15 s at 95°C and 1 min at 60°C. Quantification cycle (*Cq*) values for each gene of interest were averaged and normalized against the *Cq* value of the 16S rRNA gene. The expression of each gene was

determined by averaging three replicates. The gene expression was then calibrated/normalized against the 16S rRNA gene by using the $2^{-\Delta}\Delta CT$) method (72). The primers used are listed in Table 2.

Determination of transcription start site.

Terminal deoxynucleotidyl transferase (TdT, TaKaRa) was used to catalyze the incorporation of single deoxynucleotides (dATPs) into the 3′-OH terminus of cDNA to make the dA-tailed cDNA according to the manufacturer's protocol. Touch down and nested PCR were used to amplify the dA-tailed cDNA by using an oligo(dT) (5′-gccagtcTTTTTTTTTTTTTTTT-3′) primer and a gene-specific primer (71, 73). The PCR product was cloned into pMD18-T vector (TaKaRa, Dalian, China) for sequencing.

ACKNOWLEDGMENTS

This work was supported by the Chinese Academy of Science (grant Y15103-1-401) and a One-Hundred Scholar Award to D.Q.

We declare we have no conflicts of interest.

REFERENCES

1. Tuhela L, Carlson L, Tuovinen OH. 1997. Biogeochemical transformations of Fe and Mn in oxic groundwater and well water environments. J Environ Sci Health 32:407– 426. 2. Emerson D, Fleming EJ, McBeth JM. 2010. Iron-oxidizing bacteria: an environmental and genomic perspective. Annu Rev Microbiol 64: 561–583. https://doi.org/10.1146/annurev.micro.112408.134208. 3. Schuster J, Schafer F, Hubler N, Brandt A, Rosell M, Hartig C, Harms H, Muller RH, Rohwerder T. 2012. Bacterial degradation of tert-amyl alcohol proceeds via hemiterpene 2-methyl-3-buten-2-ol by employing the tertiary alcohol desaturase function of the Rieske nonheme mononuclear iron oxygenase MdpJ. J Bacteriol 194:972–981. https://doi.org/10.1128/ JB.06384-11. 4. Schafer F, Muzica L, Schuster J, Treuter N, Rosell M, Harms H, Muller RH, Rohwerder T. 2011. Formation of alkenes via degradation of tert-alkyl ethers and alcohols by Aquincola tertiaricarbonis L108 and Methylibium spp. Appl Environ Microbiol 77:5981–5987. https://doi.org/10.1128/AEM .00093-11. 5. Schuster J, Purswani J, Breuer U, Pozo C, Harms H, Muller RH, Rohwerder T. 2013. Constitutive expression of the cytochrome P450 EthABCD monooxygenase system enables degradation of synthetic dialkyl ethers in Aquincola tertiaricarbonis L108. Appl Environ Microbiol 79:2321–2327. https://doi.org/10.1128/AEM.03348-12. 6. Muller RH, Rohwerder T, Harms H. 2008. Degradation of fuel oxygenates and their main intermediates by Aquincola tertiaricarbonis L108. Microbiology 154:1414 –1421. https://doi.org/10.1099/mic.0.2007/014159-0. 7. Xia S, Jia R, Feng F, Xie K, Li H, Jing D, Xu X. 2012. Effect of solids retention time on antibiotics removal performance and microbial communities in an A/O-MBR process. Bioresour Technol 106:36 – 43. https:// doi.org/10.1016/j.biortech.2011.11.112. 8. Guo J, Peng Y, Yang X, Wang Z, Zhu A. 2014. Changes in the microbial community

structure of filaments and floc formers in response to various carbon sources and feeding patterns. Appl Microbiol Biotechnol 98:7633–7644. https://doi.org/10.1007/s00253-014-5805-5. 9. An W, Guo F, Song Y, Gao N, Bai S, Dai J, Wei H, Zhang L, Yu D, Xia M, Yu Y, Qi M, Tian C, Chen H, Wu Z, Zhang T, Qiu D. 2016. Comparative genomics analyses on EPS biosynthesis genes required for floc formation of Zoogloea resiniphila and other activated sludge bacteria. Water Res 102:494 –504. https://doi.org/10.1016/j.watres.2016.06.058. 10. Lechner U, Brodkorb D, Geyer R, Hause G, Hartig C, Auling G, FayolleGuichard F, Piveteau P, Muller RH, Rohwerder T. 2007. Aquincola tertiaricarbonis gen. nov., sp. nov., a tertiary butyl moiety-degrading bacterium. Int J Syst Evol Microbiol 57:1295–1303. https://doi.org/10.1099/ijs .0.64663-0. 11. Rohwerder T, Muller RH, Weichler MT, Schuster J, Hubschmann T, Muller S, Harms H. 2013. Cultivation of Aquincola tertiaricarbonis L108 on the fuel oxygenate intermediate tert-butyl alcohol induces aerobic anoxygenic photosynthesis at extremely low feeding rates. Microbiology 159: 2180 –2190. https://doi.org/10.1099/mic.0.068957-0. 12. Goris J, Konstantinidis KT, Klappenbach JA, Coenye T, Vandamme P, Tiedje JM. 2007. DNA-DNA hybridization values and their relationship to whole-genome sequence similarities. Int J Syst Evol Microbiol 57:81–91. https://doi.org/10.1099/ijs.0.64483-0. 13. Wong SM, Mekalanos JJ. 2000. Genetic footprinting with mariner-based transposition in Pseudomonas aeruginosa. Proc Natl Acad SciUSA 97:10191–10196. https://doi.org/10.1073/pnas.97.18.10191. 14. Qiu D, Eisinger VM, Head NE, Pier GB, Yu HD. 2008. ClpXP proteases positively regulate alginate overexpression and mucoid conversion in Pseudomonas aeruginosa. Microbiology 154:2119 –2130. https://doi.org/ 10.1099/mic.0.2008/017368-0. 15. Qiu D, Eisinger VM, Rowen DW, Yu HD. 2007. Regulated proteolysis controls mucoid conversion in Pseudomonas aeruginosa. Proc Natl Acad Sci U S A 104:8107– 8112. https://doi.org/10.1073/pnas.0702660104. 16. Prombutara P, Allen MS. 2015. Identification of a gene involved in flocculation by whole genome sequencing of Thauera aminoaromatica MZ1T floc-defective mutants. Appl Environ Microbiol 82:1646 –1652. https://doi.org/10.1128/AEM.02917-15. 17. Guo X, Wang X, Liu J. 2016. Composition analysis of fractions of extracellular polymeric substances from an activated sludge culture and identification of dominant forces affecting microbial aggregation. Sci Rep 6:28391. https://doi.org/10.1038/srep28391. 18. Rosenberg E, Kaplan N, Pines O, Rosenberg M, Gutnick D. 1983. Capsular polysaccharides interfere with adherence of AcinetobacterCalcoaceticus to hydrocarbon. FEMS Microbiol Lett 17:157–160. https://doi.org/10.1111/j.1574-6968.1983.tb00392.x. 19. Obuekwe CO, Al-Jadi ZK, Al-Saleh ES. 2007. Sequential hydrophobic partitioning of cells of Pseudomonas aeruginosa gives rise to variants of increasing cell-surface hydrophobicity. FEMS Microbiol Lett 270: 214 –219. https://doi.org/10.1111/j.1574-6968.2007.00685.x. 20. Yip ES, Grublesky BT, Hussa EA, Visick KL. 2005. A novel, conserved cluster of genes promotes

symbiotic colonization and sigma-dependent biofilm formation by Vibrio fischeri. Mol Microbiol 57:1485–1498. https:// doi.org/10.1111/j.1365-2958.2005.04784.x. 21. Saldias MS, Lamothe J, Wu R, Valvano MA. 2008. Burkholderia cenocepacia requires the RpoN sigma factor for biofilm formation and intracellular trafficking within macrophages. Infect Immun 76:1059 –1067. https://doi .org/10.1128/IAI.01167-07. 22. Hao B, Mo ZL, Xiao P, Pan HJ, Lan X, Li GY. 2013. Role of alternative sigma factor 54 (RpoN) from Vibrio anguillarum M3 in protease secretion, exopolysaccharide production, biofilm formation, and virulence. Appl Microbiol Biotechnol 97:2575–2585. https://doi.org/10.1007/s00253-012 -4372-x. 23. Zhao K, Liu M, Burgess RR. 2010. Promoter and regulon analysis of nitrogen assimilation factor, sigma 54, reveal alternative strategy for E. coli MG1655 flagellar biosynthesis. Nucleic Acids Res 38:1273–1283. https://doi.org/10.1093/nar/gkp1123. 24. Li R, Withers RT, Dai J, Ruan J, Li W, Dai Y, An W, Yu D, Wei H, Xia M, Tian C, Yu HD, Qiu D. 2016. Truncated type IV pilin PilA108 activates the intramembrane protease AlgW to cleave MucA and PilA108 itself in vitro. Arch Microbiol 198:885–892. https://doi.org/10.1007/s00203-016-1248-y. 25. Mattick JS. 2002. Type IV pili and twitching motility. Annu Rev Microbiol 56:289 –314. https://doi.org/10.1146/annurev.micro.56.012302.160938. 26. Burrows LL. 2012. Pseudomonas aeruginosa Twitching motility: type IV pili in action. Annu Rev Microbiol 66:493–520. https://doi.org/10.1146/ annurev-micro-092611-150055. 27. Pelicic V. 2008. Type IV pili: e pluribus unum? Mol Microbiol 68:827– 837. https://doi.org/10.1111/j.1365-2958.2008.06197.x. 28. O'Toole GA. 2011. Microtiter dish biofilm formation assay. J Vis Exp https://doi.org/10.3791/2437. 29. Pehl MJ, Jamieson WD, Kong K, Forbester JL, Fredendall RJ, Gregory GA, McFarland JE, Healy JM, Orwin PM. 2012. Genes that influence swarming motility and biofilm formation in Variovorax paradoxus EPS. PLoS One 7:e31832. https://doi.org/10.1371/journal.pone.0031832. 30. Hayrapetyan H, Tempelaars M, Nierop Groot M, Abee T. 2015. Bacillus cereus ATCC 14579 RpoN (sigma 54) is a pleiotropic regulator of growth, carbohydrate metabolism, motility, biofilm formation and toxin production. PLoS One 10:e0134872. https://doi.org/10.1371/journal.pone .0134872. 31. Ray SK, Kumar R, Peeters N, Boucher C, Genin S. 2015. rpoN1, but not rpoN2, is required for twitching motility, natural competence, growth on nitrate, and virulence of Ralstonia solanacearum. Front Microbiol 6:229. https://doi.org/10.3389/fmicb.2015.00229. 32. Kullik I, Fritsche S, Knobel H, Sanjuan J, Hennecke H, Fischer HM. 1991. Bradyrhizobium japonicum has two differentially regulated, functional homologs of the sigma 54 gene (rpoN). J Bacteriol 173:1125–1138. https://doi.org/10.1128/jb.173.3.1125-1138.1991. 33. Michiels J, Moris M, Dombrecht B, Verreth C, Vanderleyden J. 1998. Differential regulation of Rhizobium etli rpoN2 gene expression during symbiosis and free-living growth. J Bacteriol 180:3620 –3628. 34. Tian F, Yu C, Li H, Wu X, Li B, Chen H, Wu M, He C. 2015. Alternative sigma factor RpoN2 is required for flagellar motility and full virulence of Xanthomonas oryzae pv. oryzae. Microbiol Res 170:177–183. https://doi

.org/10.1016/j.micres.2014.07.002. 35. Poggio S, Osorio A, Dreyfus G, Camarena L. 2002. The four different sigma 54 factors of Rhodobacter sphaeroides are not functionally interchangeable. Mol Microbiol 46:75– 85. https://doi.org/10.1046/j.1365 -2958.2002.03158.x. 36. Merrick M, Jones DHA, Thomas CM. 1993. Location of the RpoN gene on the physical map of Escherichia coli. J Bacteriol 175:1548 –1549. https:// doi.org/10.1128/jb.175.5.1548-1549.1993. 37. Meijer WG, Tabita FR. 1992. Isolation and characterization of the Nifusvw-RpoN gene cluster from Rhodobacter-Sphaeroides. J Bacteriol 174:3855–3866. https://doi.org/10.1128/jb.174.12.3855-3866.1992. 38. Cullen PJ, Fosterhartnett D, Gabbert KK, Kranz RG. 1994. Structure and expression of the alternative sigma-factor, RpoN, in RhodobacterCapsulatus. Physiological relevance of an autoactivated Nifu2-RpoN superoperon. Mol Microbiol 11:51–65. 39. Wigneshweraraj SR, Casaz P, Buck M. 2002. Correlating protein footprinting with mutational analysis in the bacterial transcription factor sigma 54 (sigma N). Nucleic Acids Res 30:1016 –1028. https://doi.org/10.1093/ nar/30.4.1016. 40. Buck M, Gallegos MT, Studholme DJ, Guo YL, Gralla JD. 2000. The bacterial enhancer-dependent sigma (54) (sigmaN) transcription factor. J Bacteriol 182:4129 – 4136. https://doi.org/10.1128/JB.182.15.4129-4136 .2000. 41. Dong TG, Mekalanos JJ. 2012. Characterization of the RpoN regulon reveals differential regulation of T6SS and new flagellar operons in Vibrio cholerae O37 strain V52. Nucleic Acids Res 40:7766 –7775. https://doi .org/10.1093/nar/gks567. 42. Donlan RM. 2002. Biofilms: microbial life on surfaces. Emerg Infect Dis 8:881– 890. https://doi.org/10.3201/eid0809.020063. 43. Singh R, Paul D, Jain RK. 2006. Biofilms: implications in bioremediation. Trends Microbiol 14:389 –397. https://doi.org/10.1016/j.tim.2006.07.001. 44. Pratt LA, Kolter R. 1999. Genetic analyses of bacterial biofilm formation. Curr Opin Microbiol 2:598 – 603. https://doi.org/10.1016/S1369-5274 (99)00028-4. 45. Davies D. 2003. Understanding biofilm resistance to antibacterial agents. Nat Rev Drug Discov 2:114 –122. https://doi.org/10.1038/nrd1008. 46. Whiteley M, Bangera MG, Bumgarner RE, Parsek MR, Teitzel GM, Lory S, Greenberg EP. 2001. Gene expression in Pseudomonas aeruginosa biofilms. Nature 413:860 – 864. https://doi.org/10.1038/35101627. 47. Oosthuizen MC, Steyn B, Theron J, Cosette P, Lindsay D, von Holy A, Brozel VS. 2002. Proteomic analysis reveals differential protein expression by Bacillus cereus during biofilm formation. Appl Environ Microbiol 68:2770 –2780. https://doi.org/10.1128/AEM.68.6.2770-2780.2002. 48. Lappin-Scott H, Burton S, Stoodley P. 2014. Revealing a world of biofilms. The pioneering research of Bill Costerton. Nat Rev Microbiol 12:781–787. https://doi.org/10.1038/nrmicro3343. 49. Allegrucci M, Hu FZ, Shen K, Hayes J, Ehrlich GD, Post JC, Sauer K. 2006. Phenotypic characterization of Streptococcus pneumoniae biofilm development. J Bacteriol 188:2325–2335. https://doi.org/10.1128/JB.188.7 .2325-2335.2006. 50. O'Toole G, Kaplan HB, Kolter R. 2000. Biofilm formation as microbial development. Annu Rev Microbiol 54:49 –79. https://doi.org/10.1146/ annurev.micro.54.1.49. 51.

Reasoner DJ, Geldreich EE. 1985. A new medium for the enumeration and subculture of bacteria from potable water. Appl Environ Microbiol 49:1–7. 52. Fukui T, Yoshimoto A, Matsumoto M, Hosokawa S, Saito T. 1976. Enzymatic synthesis of poly-beta-hydroxybutyrate in Zoogloea ramigera. Arch Microbiol 110:149 –156. https://doi.org/10.1007/BF00690222. 53. Aziz RK, Bartels D, Best AA, DeJongh M, Disz T, Edwards RA, Formsma K, Gerdes S, Glass EM, Kubal M, Meyer F, Olsen GJ, Olson R, Osterman AL, Overbeek RA, McNeil LK, Paarmann D, Paczian T, Parrello B, Pusch GD, Reich C, Stevens R, Vassieva O, Vonstein V, Wilke A, Zagnitko O. 2008. The RAST server: rapid annotations using subsystems technology. BMC Genomics 9:75. https://doi.org/10.1186/1471-2164-9-75. 54. Wilke A, Wilkening J, Glass EM, Desai NL, Meyer F. 2011. An experience report: porting the MG-RAST rapid metagenomics analysis pipeline to the cloud. Concurrency Comput Pract Experience 23:2250 –2257. https:// doi.org/10.1002/cpe.1799. 55. Jeanmougin F, Thompson JD, Gouy M, Higgins DG, Gibson TJ. 1998. Multiple sequence alignment with Clustal X. Trends Biochem Sci 23: 403– 405. https://doi.org/10.1016/S0968-0004(98)01285-7. 56. Nicholas KB, Nicholas HB, Deerfield DW. 1997. GeneDoc: analysis and visualization of genetic variation. Embnew News 4:1. 57. Tamura K, Stecher G, Peterson D, Filipski A, Kumar S. 2013. MEGA6: molecular evolutionary genetics analysis version 6.0. Mol Biol Evol 30: 2725–2729. https://doi.org/10.1093/molbev/mst197. 58. Bouhenni R, Gehrke A, Saffarini D. 2005. Identification of genes involved in cytochrome c biogenesis in Shewanella oneidensis, using a modified mariner transposon. Appl Environ Microbiol 71:4935– 4937. https://doi .org/10.1128/AEM.71.8.4935-4937.2005. 59. Kovach ME, Elzer PH, Hill DS, Robertson GT, Farris MA, Roop RM, II, Peterson KM. 1995. Four new derivatives of the broad-host-range cloning vector pBBR1MCS, carrying different antibiotic-resistance cassettes. Gene 166:175–176. https://doi.org/10.1016/0378-1119(95)00584-1. 60. Wingender J, Strathmann M, Rode A, Leis A, Flemming HC. 2001. Isolation and biochemical characterization of extracellular polymeric substances from Pseudomonas aeruginosa. Methods Enzymol 336:302–314. https://doi.org/10.1016/S0076-6879(01)36597-7. 61. Muralidharan J, Jayachandran S. 2003. Physicochemical analyses of the exopolysaccharides produced by a marine biofouling bacterium, Vibrio alginolyticus. Process Biochem 38:841– 847. https://doi.org/10.1016/ S0032-9592(02)00021-3. 62. Dubois M, Gilles KA, Hamilton JK, Rebers PA, Smith F. 1956. Colorimetric method for determination of sugars and related substances. Anal Chem 28:350 –356. https://doi.org/10.1021/ac60111a017. 63. Hong K, Sun S, Tian W, Chen GQ, Huang W. 1999. A rapid method for detecting bacterial polyhydroxyalkanoates in intact cells by Fourier transform infrared spectroscopy. Appl Microbiol Biotechnol 51:523–526. https://doi.org/10.1007/s002530051427. 64. Ng KJ, Andresen BD, Bianchine JR, Iams JD, O'Shaugnessy RW, Stempel LE, Zuspan FP. 1982. Capillary gas chromatographic-mass spectrometric profiles of trimethylsilyl derivatives of organic acids from amniotic fluids of different gestational age. J Chromatogr

228:43–50. https://doi.org/10 .1016/S0378-4347(00)80417-X. 65. Allen MS, Welch KT, Prebyl BS, Baker DC, Meyers AJ, Sayler GS. 2004. Analysis and glycosyl composition of the exopolysaccharide isolated from the floc-forming wastewater bacterium Thauera sp. MZ1T. Environ Microbiol 6:780 –790. https://doi.org/10.1111/j.1462-2920.2004.00615.x. 66. York WS, Darvill AG, McNeil M, Stevenson TT, Albersheim P. 1986. Isolation and characterization of plant-cell walls and cell-wall components. Methods Enzymol 118:3– 40. https://doi.org/10.1016/0076-6879 (86)18062-1. 67. Tans-Kersten J, Brown D, Allen C. 2004. Swimming motility, a virulence trait of Ralstonia solanacearum, is regulated by FlhDC and the plant host environment. Mol Plant Microbe Interact 17:686 – 695. https://doi.org/10 . 1094/MPMI.2004.17.6.686. 68. Kelman A, Hruschka J. 1973. The role of motility and aerotaxis in the selective increase of avirulent bacteria in still broth cultures of Pseudomonas solanacearum. J Gen Microbiol 76:177–188. https://doi.org/10 .1099/00221287-76-1-177. 69. Rosenberg M, Perry A, Bayer EA, Gutnick DL, Rosenberg E, Ofek I. 1981. Adherence of Acinetobacter calcoaceticus RAG-1 to human epithelial cells and to hexadecane. Infect Immun 33:29 –33. 70. Zeng G, Liu Z, Zhong H, Li J, Yuan X, Fu H, Ding Y, Wang J, Zhou M. 2011. Effect of monorhamnolipid on the degradation of n-hexadecane by Candida tropicalis and the association with cell surface properties. Appl Microbiol Biotechnol 90:1155–1161. https://doi.org/10.1007/s00253-011 -3125-6. 71. Dai J, Wei H, Tian C, Damron FH, Zhou J, Qiu D. 2015. An extracytoplasmic function sigma factor-dependent periplasmic glutathione peroxidase is involved in oxidative stress response of Shewanella oneidensis. BMC Microbiol 15:34. https://doi.org/10.1186/s12866-015-0357-0. 72. Livak KJ, Schmittgen TD. 2001. Analysis of relative gene expression data using real-time quantitative PCR and the 2ΔΔCT method. Methods 25:402– 408. https://doi.org/10.1006/meth.2001.1262. 73. Mendoza-Vargas A, Olvera L, Olvera M, Grande R, Vega-Alvarado L, Taboada B, Jimenez-Jacinto V, Salgado H, Juarez K, Contreras-Moreira B, Huerta AM, Collado-Vides J, Morett E. 2009. Genome-wide identification of transcription start sites, promoters and transcription factor binding sites in E. coli. PLoS One 4:e7526. https://doi.org/10.1371/journal.pone .0007526.